

## Correlation between Adhesion Hysteresis and Phase State of Monolayer Films

Manoj K. Chaudhury\* and Michael J. Owen

Dow Corning Corporation, Midland, Michigan 48686

Received: February 8, 1993; In Final Form: March 15, 1993

Chemisorbed films of hydrolyzed hexadecyltrichlorosilane ( $\text{Cl}_3\text{Si}(\text{CH}_2)_{15}\text{CH}_3$ ) on elastomeric poly(dimethylsiloxane)s (PDMS) were used as model systems to study adhesion between polymer surfaces. The adhesion energies of these chemically modified surfaces were estimated by measuring the deformations that resulted on contacting small semispherical lenses and flat sheets of the polymer under controlled loads. The adhesion energies of these chemically modified surfaces obtained from the compressive loads were not always the same as those obtained from the decompressive loads—there was generally a finite hysteresis in adhesion energies. The magnitude of the adhesion hysteresis depends on the physical states of the alkylsiloxane films.

### Introduction

When a curved elastic solid is brought into contact with another curved or flat solid substrate, the interfacial forces acting across the interface tend to deform the solids and thus increase their area of contact. Measurement of contact deformation between elastic solids is useful in estimating their adhesion energies, which can be done using the JKR<sup>1</sup> (Johnson, Kendall, and Roberts) theory. For soft materials,<sup>1-5</sup> a lens can be placed upon another lens or flat substrate and the contact deformation can be measured directly with a microscope. For stiffer materials,<sup>6,7</sup> curved solid films are used in a cross cylinder configuration, and the contact deformation is determined using interference techniques. Based upon the well-known Derjaguin approximation, both of these geometries are amenable to the similar treatments of contact mechanics. While the traditional use of cross cylinder geometries had been restricted primarily to studies involving mica, recently it has been shown that the method is also suitable for the study of adhesion between thin films of polymers.<sup>8</sup>

Operationally, a typical experiment of contact deformation can be carried out using a strategy similar to that of measuring contact angles. The adhesion energy obtained from the compressive load is analogous to the advancement of a liquid drop on a solid surface, because in both cases the interfacial areas continue to increase. By comparison, the decompressive load-deformation experiment is analogous to the retraction of a liquid drop from a solid surface. Like the hysteresis in wetting, the adhesion energies obtained from the compressive loads are not always the same as those obtained from the decompressive loads—there is generally a finite hysteresis in adhesion energies. Dutroski<sup>2</sup> first observed hysteresis in contact deformation between a glass hemisphere and a flat slab of rubber. Recent evidence from our laboratory<sup>3,4</sup> and elsewhere<sup>7</sup> strongly indicates that the hysteresis observed at the interface of elastic solids is the result of nonequilibrium processes occurring at interfaces.

Anelastic deformations,<sup>6</sup> disentanglement and orientation of the polymer chains,<sup>5</sup> and interdigitation<sup>7</sup> of the surface functional groups are thought to be the possible contributors to adhesion hysteresis. In parallel with these macroscopic measurements, results from AFM measurements<sup>9,10</sup> have also provided evidence for adhesion hysteresis. In many of these studies, ordered monomolecular films of functional alkanes have been used as model systems. In order to rationalize the adhesion hysteresis in AFM measurements, the anelastic deformation<sup>10</sup> of the monolayer films was invoked, whereas Chen et al.<sup>7</sup> considered the possibility of interdigitation of surface functional groups as the main cause of adhesion hysteresis (Figure 1). Here, we present

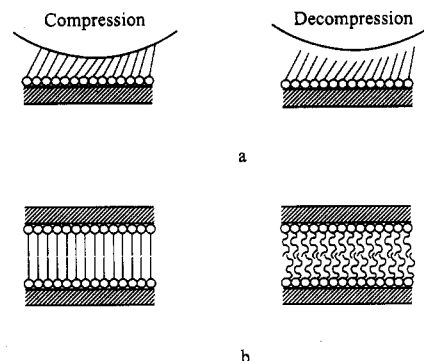


**Figure 1.** Current models of adhesion hysteresis. A model based on the stress-induced reconstruction of a self-assembled monolayer is shown in part a (see ref 10 for details). Part b depicts interdigitation of the monolayer. There is no interdigitation of the surfactant chains for the crystalline monolayers and hence there is no adhesion hysteresis. For monolayers in a glassy amorphous state interdigitation may occur, which leads to adhesion hysteresis (see ref 7 for details).

the results of a study that suggests other possible origins of adhesion hysteresis, namely those arising from the chemical heterogeneities of surfaces.

Our study used semispherical lenses and flat sheets of elastomeric PDMS as model systems. The surface properties of both the lens and flat sheets were controlled using the chemisorbed films of hexadecyltrichlorosilane (HTS). The physical state of the film was controlled by varying the surface density of HTS on PDMS. Low-density silanes exhibit a fluidlike state. As the concentration of the silane increases, the film becomes more compact and, finally, it reaches a condensed state (Figure 2). The adhesion hysteresis is shown to be profoundly influenced by the physical states of these chemisorbed layers of silanes.

### Results and Discussion

**Characterization of the Monolayers.** Self-assembled monolayers of hexadecylsiloxane were formed by exposing oxidized lenses and flat sheets of PDMS ( $\text{PDMS}^{\text{ox}}$ ) to the vapor of hexadecyltrichlorosilane (HTS) under reduced pressure. HTS chemisorbs on  $\text{PDMS}^{\text{ox}}$  by reacting with the silanols and/or adsorbed water of the surface. The resultant surface is denoted here as  $\text{PDMS}^{\text{ox}}-\text{O}_3\text{Si}(\text{CH}_2)_{15}\text{CH}_3$ . The physical states of the adsorbed silanes were inferred using infrared spectroscopy from the position<sup>11</sup> of the symmetric and asymmetric  $\text{CH}_2$  stretches. For a well-packed monolayer, asymmetric ( $\nu_a$ ) and symmetric ( $\nu_s$ )  $\text{CH}_2$  stretches were found at 2919 and 2850  $\text{cm}^{-1}$  respectively (Figure 3). For low-density monolayers, these peak positions were observed at 2925 and 2855  $\text{cm}^{-1}$ , respectively. The observed

\* Author to whom correspondence should be addressed.

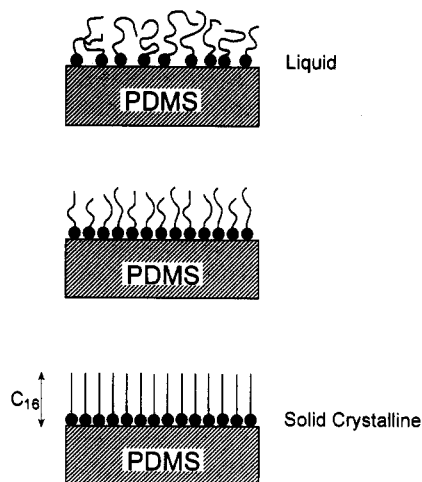


**Figure 2.** Model systems used to study adhesion hysteresis. If the surfactant is loosely packed, it is in a liquidlike state. A crystalline monolayer is formed when the molecules are in a highly compact state.

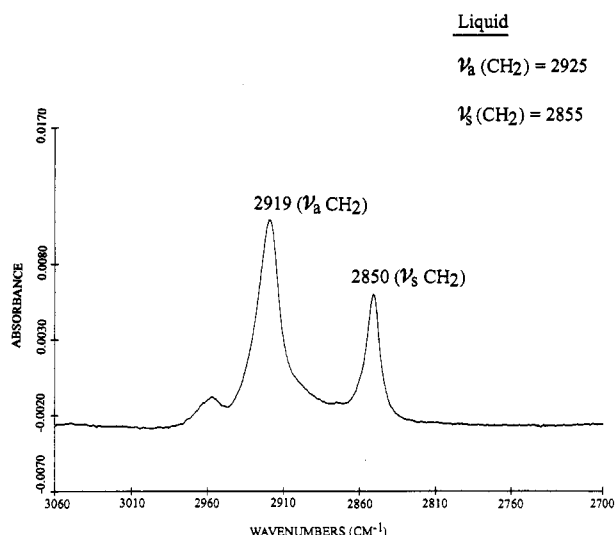


**Figure 3.** Infrared spectrum of a highly packed monolayer of hexadecylsiloxane supported on oxidized PDMS.

**TABLE I: Surface Energetics and Phase State of Monolayer<sup>a</sup>**

$\phi_s$ (%)	phase state	$\gamma_{sv}^a$ (erg/cm <sup>2</sup> )	$\gamma_{sv}^r$ (erg/cm <sup>2</sup> )	$\Delta\gamma_{sv}$ (erg/cm <sup>2</sup> )	$\Delta W_{H_2O}$ (erg/cm <sup>2</sup> )	$\Delta W_{HD}^*$ (erg/cm <sup>2</sup> )
100	solidlike	16.2	24.8	8.6	20	0
80	solid/liquid	21.5	27.6	6.1	18	0
70	liquid	23.3	23.5	0.2	8	0
60	liquid	27	28.3	1.3	12	0
40	liquid	28.5	32.8	4.3	20	0

<sup>a</sup>  $\phi_s$  represent the fractional coverage of the monolayer.  $\gamma_{sv}^a$  and  $\gamma_{sv}^r$  are the surface free energies obtained from the compressive (advancing) and decompressive (receding) load-deformation studies.  $\Delta W_{H_2O}$  and  $\Delta W_{HD}$  are the wetting hysteresis of water and hexadecane (see eq 1) on the monolayer surfaces. Since the wetting hysteresis of hexadecane is less than 1 erg/cm<sup>2</sup>, its value is shown as zero here.

upward shift (5–6 cm<sup>-1</sup>) of the CH<sub>2</sub> stretches is consistent with the value (6 cm<sup>-1</sup>) calculated by Snyder et al.<sup>11</sup> on going from an ordered to a disordered hydrocarbon chain. The wettabilities of these modified PDMS surfaces were studied using hexadecane and water as probe liquids. The values of the wetting hysteresis were determined using eq 1 and are tabulated in Table I. In eq

$$\text{wetting hysteresis} = \gamma_{lv} (\cos \theta_r - \cos \theta_a) \quad (1)$$

1,  $\theta_a$  and  $\theta_r$  are the advancing and receding contact angles,

respectively;  $\gamma_{lv}$  is the surface tension of the probe liquid. The wetting hysteresis of hexadecane on these surfaces is negligible (<1 erg/cm<sup>2</sup>) whereas the wetting hysteresis of water shows a marked dependence on the physical state of the monolayers. Large hysteresis is observed for the monolayer that is in the most compact state. In order to determine more quantitatively the degree of order exhibited by the close-packed monolayer, we have determined the dichroic ratio using p- and s-polarized IR spectroscopy.<sup>12</sup> The theoretical dichroic ratio for a close-packed monolayer with all the molecules standing perpendicular to the surface is 1.25. The similar value for a randomly oriented monolayer is 0.57. The experimentally found dichroic ratio of the well-packed monolayer is 1.17. The thickness of the monolayer on oxidized PDMS could not be determined by ellipsometry. Instead, the thickness of the equivalent monolayer as found on a polished silicon wafer was taken as an approximate estimate of the thickness of the monolayer on PDMS<sup>ox</sup>. The fractional coverages of the monolayers on PDMS<sup>ox</sup> were also determined from the estimated thicknesses obtained from the equivalent monolayers formed on polished silicon wafers. The justification for this procedure is that the surface properties of the two types of monolayers are found to be identical by infrared spectroscopy and measurements of wettabilities. We are aware that such a procedure for determining surface coverage is not rigorously correct; but it provides an approximate reference point to compare the results obtained with surfaces of different surface coverages. The thickness of the monolayer in the most compact state is about 22 Å, which is nearly the length (23.5 Å) of the HTS molecule in the trans-extended configuration. This result as well as the results obtained from IR spectroscopy indicates that the physical state of the monolayer in the most compact state corresponds, at least, to that of pseudocrystalline order.

**Adhesion Hysteresis and Phase State of Monolayer.** The deformations resulting from the contact between a semispherical lens and a flat sheet of PDMS were measured as a function of compressive and decompressive loads. The data obtained from these load-deformation studies were analyzed according to the theory of Johnson, Kendall and Roberts<sup>1</sup> to estimate the adhesion energies ( $W$ ) (eq 2). In this equation,  $a$  (cm) is the radius of the

$$a^3 = (R/K)\{P + 3\pi RW + [6\pi RPW + (3\pi RW)^2]^{0.5}\} \quad (2)$$

contact deformation,  $R$  (cm) is the radius of curvature of the lens,  $P$  (dynes) is the external load, and  $K$  (dynes/cm<sup>2</sup>) is the composite modulus. In our studies, the values of  $K$  clustered around  $4 \times 10^6$  dyn/cm<sup>2</sup>. The surface free energy  $\gamma_{sv}$  was taken as one-half of the value of  $W$  for similar surfaces.

Figures 4a and 5a–d summarize the results of contact deformations. Like the hysteresis in the contact angle of water, the most crystalline monolayer exhibits the largest adhesion hysteresis. Hysteresis decreases as the monolayer becomes more liquidlike. The surface free energies of the monolayers were calculated from the contact angles of hexadecane using the equation of Good–Girifalco and Fowkes.<sup>13</sup>

$$\gamma_{sv} = \gamma_{lv}(1 + \cos \theta)^2/4 \quad (3)$$

The surface free energy (16 erg/cm<sup>2</sup>) of the most crystalline monolayer ( $\nu_a(\text{CH}_2) = 2919$  cm<sup>-1</sup>) obtained from the compressive part of the load-deformation cycle (Figure 4a) is lower than the value (20.2 erg/cm<sup>2</sup>) obtained from the contact angle of hexadecane (45°). This lower value may be explained if the surfaces are microscopically rough. In order to test if the surface roughness has any effect on the reduction of adhesion energy, we have measured the adhesion between an HTS-coated PDMS lens and an HTS-coated, molecularly smooth, mica under conditions that were identical to those used for two PDMS surfaces. The monolayer formed on mica by the adsorption of HTS is highly ordered, as evidenced by the infrared spectroscopy ( $\nu_a(\text{CH}_2) =$

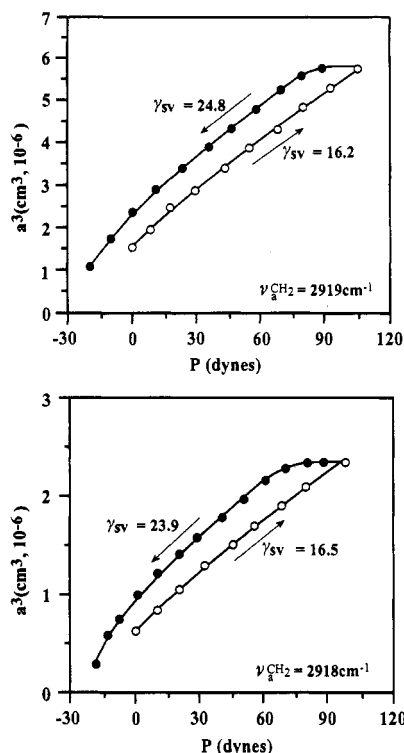


**Figure 4.** Adhesion hysteresis for crystalline monolayers. Part a (top) shows the result obtained for a semispherical lens and flat sheet of PDMS<sup>ox</sup>-O<sub>3</sub>Si(CH<sub>2</sub>)<sub>15</sub>CH<sub>3</sub>. Part b (bottom) shows the corresponding result obtained for a semispherical lens of PDMS<sup>ox</sup>-O<sub>3</sub>Si(CH<sub>2</sub>)<sub>15</sub>CH<sub>3</sub> and a flat film of mica-O<sub>3</sub>Si(CH<sub>2</sub>)<sub>15</sub>CH<sub>3</sub>. The open and closed circles represent the results obtained from the compressive and decompressive loads, respectively. The radii of the lenses used in these experiments were 0.99 mm (a) and 0.90 mm (b).

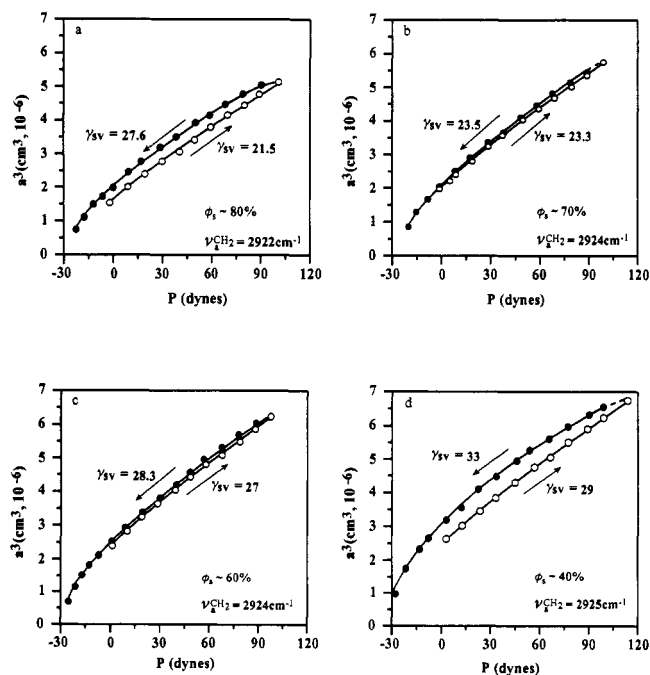


**Figure 5.** Adhesion hysteresis as a function of the physical state of HTS layer adsorbed onto PDMS<sup>ox</sup>. The open and closed symbols represent the data obtained from compressive and decompressive loads, respectively. The fractional coverages ( $\phi_s$ ) as well as the positions of the asymmetric CH<sub>2</sub> stretches for these monolayers are given. The radii of the lenses used in these experiments were 0.87 mm (a), 0.95 mm (b), 0.97 mm (c), and 0.96 mm (d).

2918 cm<sup>-1</sup>). The adhesion energies of this system are essentially the same as those of the two PDMS surfaces (compare Figure 4, a and b). Had roughness played any role, the adhesion energies

of the two systems should have differed somewhat. As this is not the case, we believe that the effect of roughness is not significant here. The following results further support this view.

For a slightly more disordered monolayer ( $\phi_s = 80\%$ ;  $\nu_a(\text{CH}_2) = 2922 \text{ cm}^{-1}$ ), the surface free energy from the contact angle of hexadecane ( $40^\circ$ ) is  $21.6 \text{ erg/cm}^2$ , which agrees well with the compressive part of the load-deformation experiment. The  $\gamma_{sv}$  value ( $27.6 \text{ erg/cm}^2$ ) obtained from the decomposition experiment is somewhat higher than the value obtained from contact angle. For a more disordered liquidlike monolayer ( $\phi_s = 70\%$ ,  $\nu_a(\text{CH}_2) = 2924 \text{ cm}^{-1}$ ), adhesion hysteresis is negligible, with the  $\gamma_{sv}$  values obtained from the JKR measurements ( $23.3 \text{ erg/cm}^2$ ) agreeing well with the value estimated from the contact angle of hexadecane ( $\theta = 38^\circ$ ;  $\gamma_{sv} = 22 \text{ erg/cm}^2$ ). For an even more disordered monolayer ( $\phi_s = 60\%$ ,  $\nu_a(\text{CH}_2) = 2924 \text{ cm}^{-1}$ ) exhibiting very low hexadecane contact angle ( $18^\circ$ ), the agreement between the two different measurements is still reasonable ( $27\text{--}28 \text{ erg/cm}^2$  from JKR;  $\gamma_{sv} = 26.5 \text{ erg/cm}^2$  from contact angle).

The good agreement between the adhesion energies obtained from the contact deformations and contact angles for surfaces exhibiting negligible adhesion hysteresis assures us that the surfaces are devoid of gross imperfections of the type that prevent molecular contact. As the surface coverage becomes too dilute ( $\phi_s = 40\%$ ), the hysteresis loop opens again. The surface free energy of this surface obtained from the compressive loads is found to be that of a pure methylene surface.<sup>14</sup> The finite adhesion hysteresis at this surface coverage reflects that the surface is heterogeneous and the bare patches of the two surfaces sense each other.

From these results we can make several generalizations. Firstly, a liquidlike monolayer does not contribute significantly to the hysteresis of contact deformations. Secondly, the hysteresis increases as the monolayer becomes crystalline. Thirdly, because of the high degree of crystallinity, it is unlikely that the hysteresis in the most compact state is due to the interdigitation of the monolayers; other possible causes of hysteresis must be sought.

**Stress-Induced Reconstruction of the Monolayer.** Joyce et al.<sup>10</sup> have recently carried out experiments on the adhesion between a tungsten tip and alkanethiol-modified gold substrates using an interfacial force microscope. They also found finite hysteresis in adhesion when the gold surface was modified with a highly dense monolayer of *n*-hexadecanethiol. The authors ascribed this adhesion hysteresis to the mechanical compaction of the monolayers and slow strain recovery (Figure 1a). However, recent Monte Carlo (MC) simulation<sup>15</sup> shows that a mechanically compacted *n*-hexadecanethiol monolayer relaxes almost elastically when the applied stress is removed. This MC simulation was, however, performed for uniform compression across the interface; in reality, there is a gradient in stress. This stress gradient may cause irreversible changes in the interfacial properties in some systems. On the basis of the following analysis, we argue that the mechanical compaction is not a significant factor for the hysteresis observed in our system.

The distribution of the normal stress<sup>7</sup> ( $\sigma(x)$ ) in the zone of contact between PDMS lens and PDMS sheet was calculated according to eq 4 and is plotted in Figure 6b. In eq 4,  $x = r/a$ ,

$$\sigma(x) = (3Ka/2\pi R)((1-x^2)^{0.5}) - ((3\gamma K/\pi a)^{0.5})((1-x^2)^{-0.5}) \quad (4)$$

$r$  is the distance from the center of the contact circle toward the edge of contact (see Figure 6a).

The central part of the contact area is under a compressive stress. The stress becomes tensile at a distance of about 90% from the center to the edge of contact. If the stress-induced compaction of the monolayer is the primary cause of adhesion hysteresis, then the unloading branch of the load-deformation cycle should start out being reversible and then branch out from

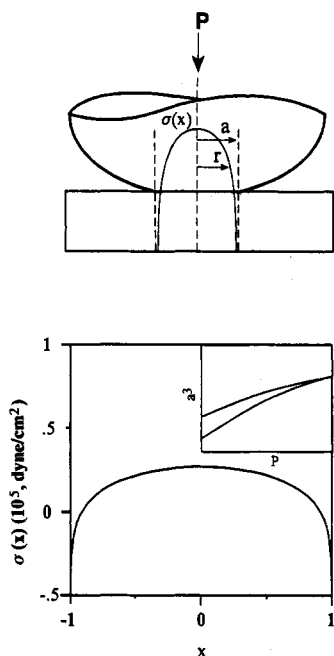


**Figure 6.** Distribution of normal stress at the interface of a semispherical lens and a flat sheet of PDMS. The stress is compressive at the center and tensile near the edge. In the inset of part b is shown the typical adhesion hysteresis loop that can be expected if the stress-induced compaction (see Figure 1a) is the primary cause of adhesion hysteresis.

the compressive curve after the radius has fallen by about 10% (see the inset of Figure 6b). The decompressive load-deformation data could not then be explained with a single value of adhesion energy (or a single value of elastic modulus). The actual load-deformation data of the unloading branch, however, deviate significantly from this prediction. Hysteresis is observed even from the early stage of unloading. The decompressive branch of the load-deformation cycle could be explained satisfactorily with a single value of surface energy. The modulus obtained from the decompressive branch deviates by only 2–3% from that obtained from the compressive branch of the load-deformation cycle. On the basis of this analysis, we do not think that the stress-induced reconstruction of the monolayer is a significant cause of adhesion hysteresis.

**Adhesion Hysteresis and Surface Heterogeneity.** The parallelism between the adhesion hysteresis in the JKR measurements and the wetting hysteresis of water is noteworthy. Equally so is the fact that the adhesion hysteresis has no direct correlation with the wetting hysteresis of hexadecane. Since water senses heterogeneities on a surface more than a nonpolar liquid,<sup>16</sup> the molecular origin of adhesion hysteresis is possibly related to the heterogeneous character of the surface. The origin of chemical heterogeneities at a low surface coverage ( $\phi_s = 40\%$ ) is obviously due to the exposure of bare silica patches. Note that the adhesion hysteresis on this surface is less sensitive to surface heterogeneity than the wetting hysteresis of water (Table I). This is so because water can sense the polar sites by migration; but the close contact between the polar sites of solids is hindered sterically by the adsorbed silanes.

The origin of heterogeneity for the compact monolayer is less obvious. We can only suggest a few possibilities. A heterogeneous surface may result in the pseudocrystalline state if the silanes adsorb on the surface as clusters. During a vapor-phase adsorption, the progression toward the equilibrium state will be dramatically slowed down during the final stages of adsorption, because the elimination of gauche defects will be thwarted by steric constraints. Several coexisting nonequilibrium phases of varying surface energies may thus form on the surface. Line defects are expected to develop for this sort of organization. Point defects may also result if some of the HTS molecules are inversely

inserted. In a pseudocrystalline or glassy environment such an erroneous configuration may be kinetically frozen. These line or point defects may act to pin the contact line and deform it about the defect sites, leading to a hysteresis in adhesion.<sup>17</sup> Liquidlike monolayers, which do not form frozen domains, but cover the surface well, relax rapidly and thus exhibit no appreciable adhesion hysteresis (Figure 5, b and c).

### Summary and Conclusions

This study provides further evidence that self-assembled monolayers of alkylsiloxane supported on oxidized PDMS are excellent model systems with which to study adhesion between surfaces. Studies of contact deformations as a function of the phase state of the monolayers provide information about adhesion at the molecular level that are complementary to contact angles. The major finding of the current study is that the interaction between solid materials, in general, has a hysteretic component, indicating that the solid–solid interfaces are in nonequilibrium (or metastable) energy states. The hysteresis observed in our adhesion studies does not conform with the models based on stress-induced reconstruction of the structure of the monolayer or the interdigitation of alkyl chains. The unimportance of the stress-induced reconstruction of the compact monolayers in adhesion hysteresis is also supported by recent MC simulations.<sup>15</sup>

The effect of stress may, however, be important in some special cases involving partially formed monolayers, where interfacial compression might force the alkyl chains adsorbed on two surfaces to interdigitate. This type of interdigitation was thought by Chen et al.<sup>7</sup> to be primary cause of adhesion hysteresis for some partially formed LB films supported onto mica. The compressive stress developed at the interface of a lens and a flat sheet of PDMS is, however,  $10^5$  times smaller than that developed at the interface of two mica cylinders. Thus, the stress-induced interdigitation of alkyl chains is of much lesser significance for the PDMS elastomers than is the case with the mica cylinders.

The high adhesion hysteresis observed in the most compact state of the monolayer argues against the interdigitation of the alkyl chains. The hysteresis, in this case, appears to be controlled by defects of the type that give rise to hysteresis in contact angles. The parallelism between adhesion hysteresis and the wetting hysteresis of water supports this view. We believe that this model, correlating heterogeneity and hysteresis, can be tested rigorously by introducing artificial defects in the monolayer structure. Studies along this direction are now being carried out in our laboratory.

### Experimental Section

**General.** Poly(dimethylsiloxane) (Dow Corning Syl-170) was supplied by Dow Corning Corp., Midland, MI. HTS (>97%) was obtained from Petrach. The liquids used to measure contact angles were water and hexadecane. Water was doubly distilled and deionized and had a surface tension of 72.8 dyn/cm. Hexadecane was purified by passing it through a column of neutral-grade alumina. The measured surface tension of hexadecane was 27.6 dyn/cm. The microsyringes (Gilmont) used to measure contact angles and to prepare PDMS lenses were obtained from VWR. Plasma oxidation was carried out in a Harrick Plasma Cleaner (Model PDC-23G, 100 W). Contact angle measurements were carried out using a Ramé Hart goniometer (Model 100). The microscope used to measure contact deformation was purchased from Nikon (Nikon Diaphot inverted microscope) and was equipped with a video camera, a video monitor, and a still camera. Infrared spectra were obtained with a Nicolet FTIR spectrometer (20 DXB). The internal reflection FTIR accessories were obtained from Harrick Corp.

**Preparation of Semispherical Lenses and Flat Sheets of PDMS.** The components for preparing the elastomers were supplied in two parts, Dow Corning Syl-170A and Syl-170B (Midland, MI). These two parts comprise the components of a reaction mixture

having vinyl end-capped oligomeric dimethylsiloxane as the major component, a methylhydrosiloxane as cross-linking agent, and a platinum (no. 2) complex as a catalyst for the hydrosilation reaction. As obtained, these components both contained fillers. Upon storage the fillers sedimented down. The clear components were poured out of the containers. Earlier, we used a 50:50 mixture (W:W) of the two clear components to prepare the cross-linked network. However, we found that occasionally some unreacted PDMS bloomed onto the surface after several days of storage. In the present study, we used a 1:3 (w:w) ratio of Syl-170A and Syl-170B. No surface blooming occurred when the networks were prepared in this manner. The effective value of  $K$  for this mixture was found to be  $4 \times 10^6$  dyn/cm<sup>2</sup>, which is slightly lower than the value ( $5 \times 10^6$  dyn/cm<sup>2</sup>) obtained previously. The mixture was stirred in a plastic weighing cup using a glass rod. Trapped air bubbles resulting from the agitation of the mixture were removed by applying gentle vacuum (60–70 mmHg for about 30 min). Small drops ( $\approx 1 \mu\text{L}$ ) of the transparent mixture were applied using a microsyringe to the surface of a smooth glass microscope slide, which had previously been treated with  $\text{Cl}_3\text{Si}(\text{CH}_2)_2(\text{CF}_2)_7\text{CF}_3$  to reduce its adhesion. The hydrosilation polymerization reaction was carried out at 65 °C for 1 h. The radii of curvature of the cured drops were measured directly at a point as close as possible to their vertex. The prepared lenses had radii of curvatures of  $\approx 1$  mm. A cured lens could be easily removed from the glass slide and manipulated by holding it at its edge by a fine-pointed tweezer. The flat sheets of silicone elastomer (thickness 1.5 mm) were prepared from the same materials as those used in preparing the lenses. These sheets were obtained by curing the two-component reaction mixture in a flat-bottomed polystyrene Petri dish. The surfaces of the sheet that were exposed to air during curing were the ones contacted with the lens during the deformation experiments.

**Apparatus Used To Measure Contact Deformation.** A detailed description of the apparatus used to measure contact deformation as a function of external load has been reported separately.<sup>3</sup> The lens could be brought slowly on or detached slowly from the flat sheet of PDMS using a micromanipulator. The flat sheet of PDMS rested on one end of a lever arm whose other end was connected to an electrobalance. Any excess load applied on the lens during the course of a load-deformation experiment was registered on the electrobalance, which had a sensitivity of 1 dyn. The lens could be brought into contact with the flat sheet at zero load by careful operation of the manipulator. The area of contact was measured by an inverted microscope (Nikon, Diaphot) which was equipped with a video camera and a video monitor. All the measurements of contact deformations were made directly from the video screen. The working distance from the stage to the condenser was 20.5 mm, which gave enough room for manipulating the specimens.

**Procedure. Measurements of Contact Deformations.** In order to carry out a load-deformation experiment, a lens ( $R \approx 1$  mm.) was brought into contact with a flat sheet of PDMS in air. Neither the temperature nor the humidity of the room was controlled. The average temperature and humidity of the laboratory were 23 °C and 50%, respectively. After the lens was contacted on the flat sheet very carefully, the contact deformation was measured. Additional load was applied by pressing the lens against the flat sheet. After the load reached a steady value, the contact deformation was again measured. The load was increased from a zero value to about 100 dyn, and the deformations were measured at random intervals. At the end of this experiment, the load was removed stepwise and the deformation was measured until the lens separated from the flat sheet.

**Measurements of Contact Angles.** Water and hexadecane were used for the contact angle measurements. Quasistatic advancing and receding contact angles were measured according to the method of Good and Neumann.<sup>18</sup> Following this technique, small liquid drops of about 1–2  $\mu\text{L}$  were formed on the solid surface using a microsyringe. While the drop was still in contact with the syringe needle, additional liquid was added to the drop to advance the drop edge as slowly as possible. After the cessation of the movement of the three-phase contact line, the advancing contact angle was measured. Receding contact angles were measured following the same procedure after withdrawing the liquid from a previously advanced drop.

**Infrared Spectroscopy.** Monolayer-coated PDMS sheets are gently placed on a silicon ATR prism and 1000 scans were collected. The IR spectrum of the silane layer was obtained by a spectral subtraction procedure using an oxidized PDMS sheet as a reference.

**Functionalization of PDMS.** The surface of PDMS was modified chemically using the basic procedure described in refs 3 and 4. Oxidation of PDMS in oxygen plasma (45 s, 0.2 Torr) resulted in a thin silica-like layer, which was further modified by reacting it with the vapor of hexadecyltrichlorosilane under reduced pressure. In a typical adsorption experiment, the samples of oxidized PDMS were placed inside a desiccator at a distance of about 1.5 cm from the silane source, and the desiccator was evacuated to about 0.001 Torr for about 15 min. The silane source was either neat liquid of HTS or HTS dissolved in paraffin oil. The concentration of the adsorbed silane onto PDMS<sup>ox</sup> was controlled by varying the concentration of the silane in the vapor phase. The following concentrations yielded monolayers of varying surface coverages: neat silane ( $\phi_s = 100\%$ ); 200  $\mu\text{L}$  of silane/3 g of paraffin oil ( $\phi_s = 80\%$ ); 100  $\mu\text{L}$  of silane/3 g of paraffin oil ( $\phi_s = 70\%$ ); 30  $\mu\text{L}$  of silane/3 g of paraffin oil ( $\phi_s = 60\%$ ); 20  $\mu\text{L}$  of silane/3 g of paraffin oil ( $\phi_s = 40\%$ ).

## References and Notes

- (1) Johnson, K. L.; Kendall, K.; Roberts, A. D. *Proc. R. Soc. London* **1971**, *A324*, 301.
- (2) Dutrowski, R. C. *Trans. ASME, J. Lubr. Technol.* **1969**, *91F*, 732.
- (3) Chaudhury, M. K.; Whitesides G. M. *Langmuir* **1991**, *7*, 1013.
- (4) Chaudhury, M. K.; Whitesides, G. M. *Science* **1992**, *255*, 1230.
- (5) Shanahan, M. E. R.; Michel, F. *Int. J. Adhesion Adhesives*. **1991**, *11* No. 3, 170.
- (6) Horn, R. G.; Israelachvili, J. N.; Pribac, F. *J. Colloid Interface Sci.* **1987**, *115*, 480.
- (7) Chen, Y. L.; Helm, C. A.; Israelachvili, J. N. *J. Phys. Chem.* **1991**, *95*, 10737.
- (8) Merrill, W. W.; Pocius, A. V.; Thakkar, B. V.; Tirrell, M. *Langmuir* **1991**, *7*, 1975.
- (9) Burnham, N. A.; Dominguez, D. D.; Mowery, R. L.; Colton, R. J. *Phys. Rev. Lett.* **1990**, *64*, 1931.
- (10) Joyce, S. A.; Thomas, R. C.; Houston, J. E.; Michalske, T. A.; Crooks, R. M. *Phys. Rev. Lett.* **1992**, *68*, 2790.
- (11) Snyder, R. G.; Strauss, H. L.; Elliger, C. A. *J. Phys. Chem.* **1982**, *86*, 5145.
- (12) The dichroic ratios were calculated according to the equations developed by Harrick (Harrick, N. J. *Internal Reflection Spectroscopy*; Harrick Scientific Corp., 1979; pp 17, 51). The refractive indices for silicon (IRE), monolayer, and PDMS used to calculate dichroic ratios were 3.42, 1.5, and 1.4, respectively.
- (13) Girifalco, L. A.; Good, R. J. *J. Phys. Chem.* **1957**, *61*, 904. Good, R. J.; Girifalco, L. A. *J. Phys. Chem.* **1960**, *64*, 561. Fowkes, F. M. *Ind. Eng. Chem.* **1964**, *56*, 40.
- (14) Zisman, W. A. *Adv. Chem. Ser.* **1964**, No 43, 1.
- (15) Siepmann, J. I.; McDonald, I. R. *Phys. Rev. Lett.* **1993**, *70*, 453.
- (16) Good, R. J.; Koo, M. N. *J. Colloid Interface Sci.* **1979**, *71*, 283.
- (17) Joanny, J. F.; de Gennes, P. G. *J. Chem. Phys.* **1984**, *81*, 552.
- (18) Neumann, A. W.; Good, R. J. In *Surface and Colloid Science*; Good, R. J., Stromberg, R. A., Eds.; Plenum Press: New York, 1979; Vol. 11, p 31.